ISSN: 0067-2904
GIF: 0.851

Simulation of Fraunhofer Diffraction for Plane Waves using Different Apertures

Uday. E. Jallod *

Department of Astronomy and Space, College of Science, University of Baghdad, Baghdad,Iraq .

Abstract:

In this paper a two dimensional numerical simulation have been applied using MATLAB program for generating Fraunhofer diffraction pattern from different apertures. This pattern is applied for three types of apertures, including, circular, square, and rectangular functions, and it's could be generated any wavelength in the visible light. The studying demonstrated the capability and the efficiency of optical imaging systems to observe a point source at very long distance. The circular aperture shows better results across the shape of Fraunhofer pattern and optical transfer function (*otf*). Also, the minimum values of the normalized irradiance of different diffracted apertures have been computed at different dimensions of these apertures, and found that the smallest value belongs to the circular aperture and equal to (1.0×10^{-8}) at radius (R=60 pixel).

Keywords: Fraunhofer diffraction, Fourier transform, and optical physics.

محاكاة حيود فرانهوفر للموجات المستوية باستخدام فتحات مختلفة

عدي عطيوي جلود

قسم الفلك والفضاء، كلية العلوم، جامعة بغداد، بغداد, العراق

الخلاصة:

في هذا البحث طبقت محاكاة عددية ذات بعدين باستخدام برنامج الماتلاب لتوليد نموذج فرانهوفر للحيود ولفتحات مختلفة. طبق هذا النموذج لثلاث فتحات تتضمن دوال الدائرة، المربع، والمستطيل ويمكن توليده لاي طول موجي في الضوء المرئي. بينت الدراسة القدرة والكفاءة لانظمة التصوير البصرية لرصد مصدر نقطي عند مسافة بعيدة جداً . اظهرت الفتحة الدائرية افضل النتائج عبر شكل نموذج فرانهوفر ودالة التحويل البصرية.فضلاً عن ذلك حسبت اقل قيمة للشدة المعايرة لحيود الفتحات وعند ابعاد مختلفة ووجد ان اقل قيمة تعود للفتحة الدائرية وتساوي (1.0×10^{-8}) عند نصف قطر(R=60) بكسل.

*Email:udayjallod@yahoo.com

1. Introduction:

In order to obtain a high resolution image in different fields such as astronomy, optical physics, and the high resolution object identification [1]. It should be taken in accounts several basic principles, but the most important principle is the diffraction which is build upon the shape and size of the aperture of imaging systems. There are many theories that explain diffraction phenomena; the simplest one is the Huygens – Fresnel theory. This theory assumes that a wavefront may be considered to emit secondary wavefronts as passing through the aperture. These secondary wavefronts were postulated by Christian Huygens in 1678 in Holland. Many years later, in 1815 in France, Agoustin Arago Fresnel considered that Huygens wavefronts must interfere with their corresponding phase when arriving at observing screen [2]. Diffraction could be tackled by starting with Helmholtz equation and then converting it to an integral equation using Green's theory [3].

Many other theories have been postulated to improve the diffraction. The best of them is the scalar diffraction theory that could be utilized when the wavelength of the wave is larger than of the aperture size for the optical imaging systems [4]. There are two approaches of the scalar diffraction theory which is classified into near and far field approximations according to the distance between the source and the observation plane. If this distance is infinitely large, so, the waves that arrive the aperture are considered plane waves. This is called far field approximation; therefore, the Fraunhofer diffraction pattern has been happened. The mathematical representation of far field approximation and Fraunhofer diffraction integral are the same. In contrast, the distance is large but finite; the mathematical equations of near approximation and Fresnel diffraction integral are the same [5]. Plenty of studies in the literatures that interest of this problem, which are adopting of the Fraunhofer diffraction patterns shape [6, 7].

In this paper, the mathematical equations that compute Fraunhofer diffraction integral have been studied and simulated in order to demonstrate the essential features of this pattern due to used different apertures. The minimum values of the normalized different diffracted apertures have been calculated to illustrate the ability of these apertures to resolve the point source. The optical transfer function (*otf*) has been simulated that is associated with different diffracted apertures in order to determinate the quality of the optical imaging system.

2. Theoretical Considerations:

Assuming distant quasi monochromatic waves of a point source of unity magnitude that is presented by [8]:

$$U(\eta,\gamma) = A(\eta,\gamma)e^{i\phi(\eta,\gamma)} \tag{1}$$

where A is the amplitude of the wave, η,γ is the spatial variables, consider the point source generates plane waves that pass in a homogenous medium without any perturbations, this means that the phase of the wave $\phi(\eta,\gamma)=0$ and $U(\eta,\gamma)=1$. When a plane wave passes through the aperture of imaging system the diffraction phenomena occurs. The theory of the diffraction is built on the assumption, that incidents the wave is transmitted without change at points within aperture. According to this assumption $U(\eta,\gamma)$ and $f(\eta,\gamma)$ are complex wave and could be written as [9]:

$$f(\eta,\gamma) = U(\eta,\gamma)p(\eta,\gamma) \tag{2}$$

where

$$p(\eta,\gamma) = \begin{cases} 1 & \text{inside the aperture} \\ 0 & \text{outside the aperture} \end{cases} \tag{3}$$

p is called the aperture function, but here the phase forms associated with an optical imaging system could be a function of transverse positions η,γ as given by [10]:

$$\vartheta(\eta,\gamma)=\exp\left[j\frac{k}{2z}(\eta^2+\gamma^2)\right] \tag{4}$$

where ($k=\frac{2\pi}{\lambda}$) is the wave number, λ is the wavelength and z is the propagation direction.

All apertures of the optical imaging systems are shift-invariant because of the invariance of free space to displacement of the coordinates system. A linear shift-invariant system is characterized by it's impulse response function. Impulse response function is the response of the system to an impulse or a point at the input plane. The impulse response function in far field approximation is given by [10]:

$$h(\eta,\gamma)=\frac{\exp(jkz)}{j\lambda z}\exp\left[j\frac{k}{2z}(\eta^2+\gamma^2)\right] \tag{5}$$

The Fourier transform of above equation is called transfer function and could be written as [10]:

$$H(x,y)=e^{jkz}\exp\left[j\pi\lambda z(x^2+y^2)\right] \tag{6}$$

the x & y are variables at the output plane. The transfer function is the factor by which an input function is multiplied with it's to yield the out function.

Now, the result in the Fraunhofer diffraction expression is obtained as [10]:

$$g(x,y)=\frac{\exp(jkz)}{j\lambda z}\exp\left[j\frac{k}{2z}(\eta^2+\gamma^2)\right]\times\iint f(\eta,\gamma)\exp\left[j\frac{2\pi}{\lambda z}(x\eta+y\gamma)\right]d\eta d\gamma \tag{7}$$

This equation could be obtained by applied Fourier convolution theory as:

$$g(x,y)=\Im^{-1}\{\Im\{h(\eta,\gamma)\}\Im\{f(\eta,\gamma)\}\} \tag{8}$$

where $\Im^{-1}$ is the inverse Fourier transform, $\Im$ is the Fourier transform.

Therefore, one could be writing above equation as:

$$g(x,y)=H(x,y)\otimes F(x,y) \tag{9}$$

where $\otimes$ is convolution operator, $H(x,y)$ and $F(x,y)$ are complex Fourier transform respectively of impulse response function $h(\eta,\gamma)$ and exit wave from the aperture $f(\eta,\gamma)$. Equations (8) and (9) are equivalent and representing convolution equation. Equation (7) could be written in terms of Bessel function as [10]:

$$g(x,y)=\left(\frac{w^2}{\lambda z}\right)^2\left[\frac{J_1(2\pi f(\eta,\gamma))}{\frac{w}{\lambda z}f(\eta,\gamma)}\right] \tag{10}$$

where w is the dimension (length or radius) of square, rectangular, and circular apertures. J_1 is the Bessel function of first order, equation (10) could be derived from Henkel transform.

3. Simulated Results:

The aperture function has been simulated in different shapes (circular, square, and rectangular) in size of 256 by 256 pixels with phase form as given in equation (4). Firstly, the most basic shape

aperture of the optical system is a circular function that has unity magnitude of radius (R) equal to (20) pixels according to the following equation [11]:

$$p_c(\eta,\gamma)=\begin{cases}1 \text{ if } \sqrt{(\eta-\eta_c)^2+(\gamma-\gamma_c)^2}\le R\\ 0 \text{ otherwise}\end{cases} \tag{11}$$

(η_c, γ_c) is the center of a two – dimensional array. Secondly, the square function of length (L) equal to (20) pixels has unity magnitude that is given by [12]:

$$p_s(\eta,\gamma)=\begin{cases}1 \text{ if } |\eta|\le L \,\&\, |\gamma|\le L\\ 0 \text{ otherwise}\end{cases} \tag{12}$$

Finally, the rectangular function has been taken in account in order to demonstrate the difference of the diffraction pattern with these apertures. The rectangular function has unity magnitude of length (a) that is equal to (20) pixels with wide equal to (a/2) according to the equation [13]:

$$p_r(\eta,\gamma)=\begin{cases}1 \text{ if } |\eta|\le a \,\&\, |\gamma|\le a/2\\ 0 \text{ otherwise}\end{cases} \tag{13}$$

A wave $U(\eta,\gamma)$ that given in equation (1) is transmitted through these apertures, that have amplitude transmittance as given in equations (11, 12, and 13), generating a complex wave as equation (2). Now, the Fraunhofer diffraction pattern that given in equation (7) have been computed in these different apertures with the following parameters (λ = 450 nm) the green light (or could be taken any wavelength in the visible light), and $k = 2\pi/\lambda$. In our simulations, the normalized intensity distribution of this pattern computed by taken the fast Fourier transform of these apertures then multiplied by impulse response function according to equation (7). The impulse response function should be taken in the same size of the aperture function. The results have been simulated that are demonstrated in figures -(1, 2, and 3).

The minimum value of the normalized intensity distribution inside the aperture could be calculated via

$$g(x,y)_{\min}=Min\left[\frac{g(x,y)}{g(0,0)}\right] \tag{14}$$

where $g(0,0)$ is the maximum value of the $g(x,y)$ which is located at the center of the array. The above equation has been applied for three different diffracted apertures at different dimensions (radius or length 20, 40, and 60 pixels) of these apertures.

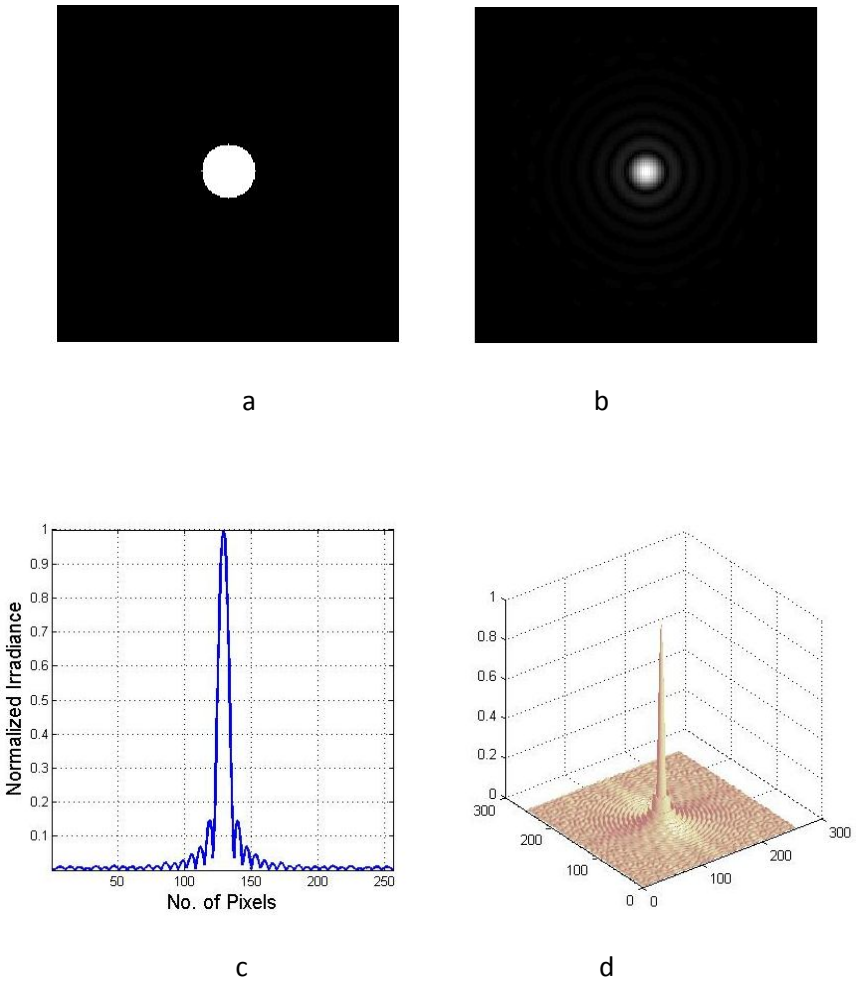

Figure 1- (a) Circular aperture, b-Fraunhofer diffraction pattern for (a), c- Central cross –section through (b), and d- Surface plot of (b).

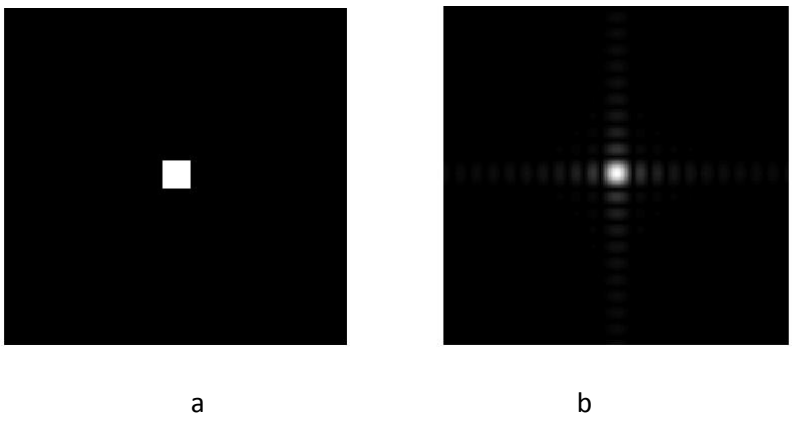

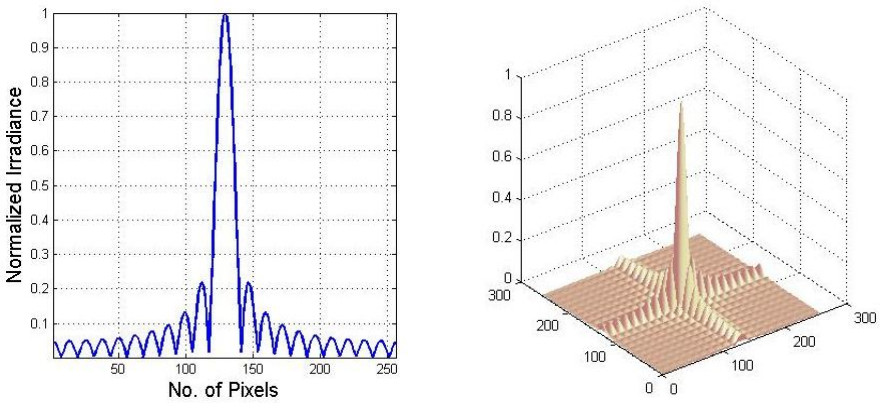

Figure 2- (a) Square aperture, b - Fraunhofer diffraction pattern for (a), c – Central cross – section through (b), and d - Surface plot of (b).

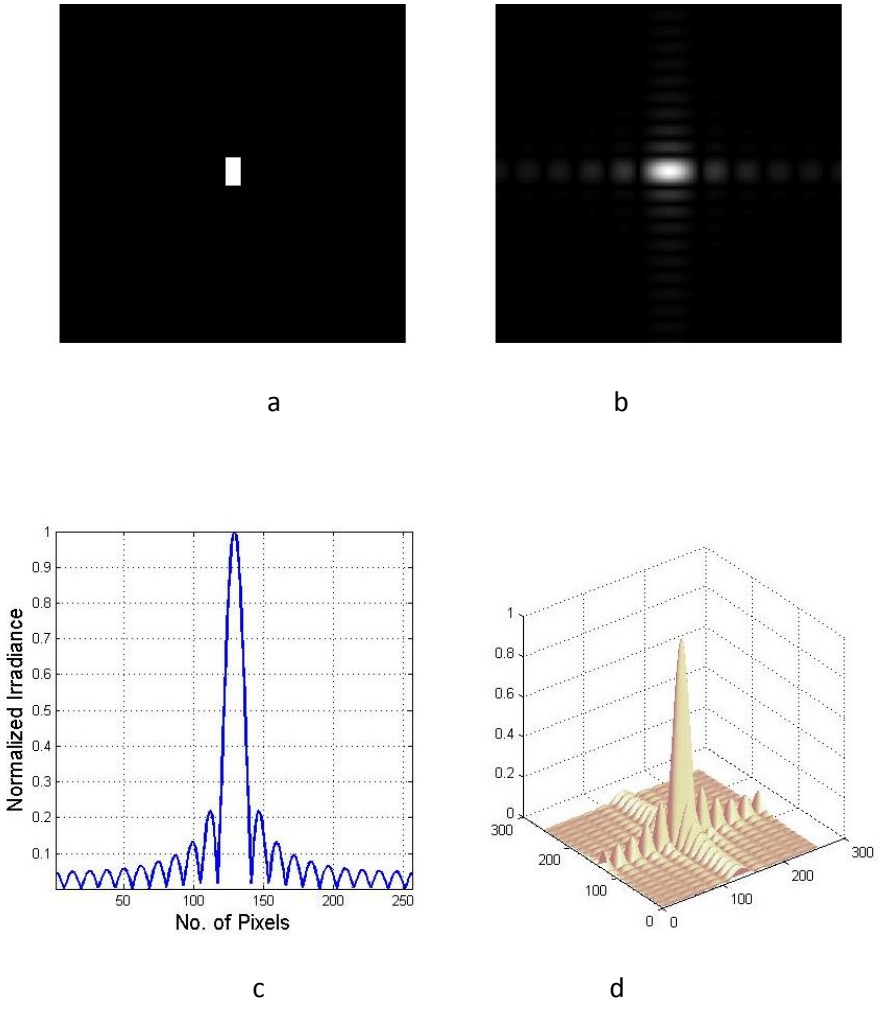

Figure 3- (a) Rectangular aperture, b- Fraunhofer diffraction pattern for (a), c- Central cross – section through (b), and d- Surface plot of (b).

In order to examine the efficiency of the optical imaging system, the optical transfer function (*otf*) has been simulated. *otf* is a measure of the imaging quality and represents how each spatial frequency components in object intensity that is transferred to the image. The normalize *otf* is given by [14]:

$$otf(u,v) = \frac{\iint p(\eta,\gamma)p^*(\eta-\lambda fu,\gamma-\lambda fv)d\eta d\gamma}{\iint |p(\eta,\gamma)|^2 d\eta d\gamma} \tag{15}$$

where f is the focal length of these lenses of the optical imaging system and the symbol $*$ indicate to the complex conjugate function. This equation is applied in the same three different diffracted apertures using convolution equation between these apertures and their complex conjugate apertures. Then normalized to their maximum values and absolute values are taken for *otf* at the same dimension which equal to 20 pixels. The results are illustrated in figure (4).

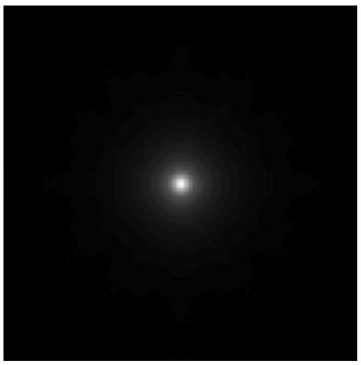

a

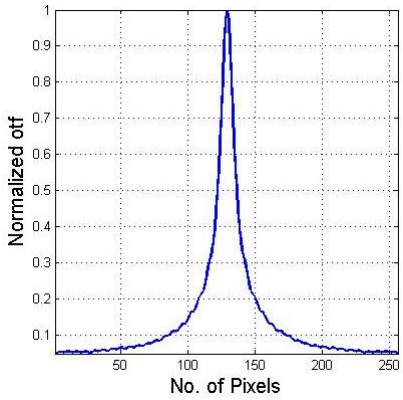

b

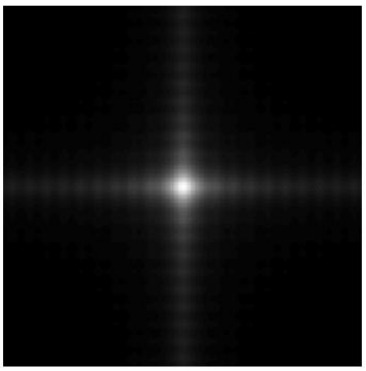

c

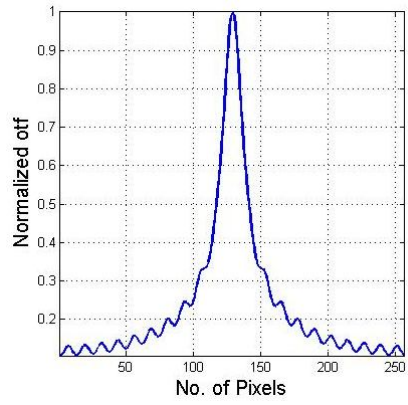

d

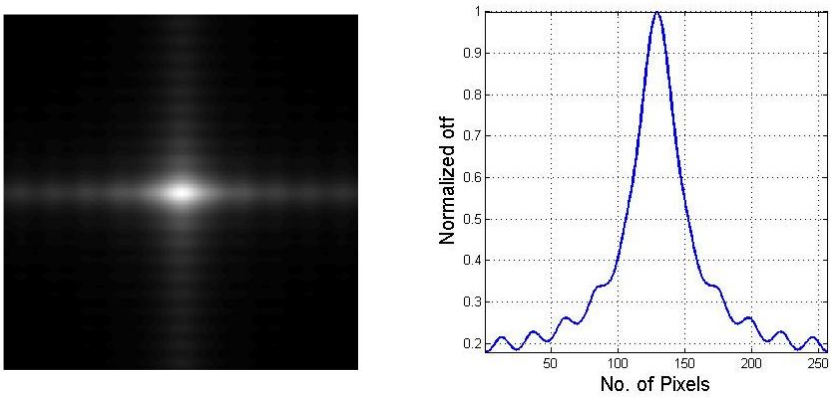

e f

Figure 4- (a) Normalized *otf* for diffracted circular aperture, b- Central line through (a),c- Normalized *otf* for diffracted square aperture, d- Central line through (c), e -Normalized *otf* for diffracted rectangular aperture, and f- Central line through (e).

It should be pointed out here that the central line through the normalized *otf* functions for different diffracted apertures at the minimum and the best dimensions which equal to (20 and 60 pixels) respectively are simulated, as illustrated in figures (5 & 6).

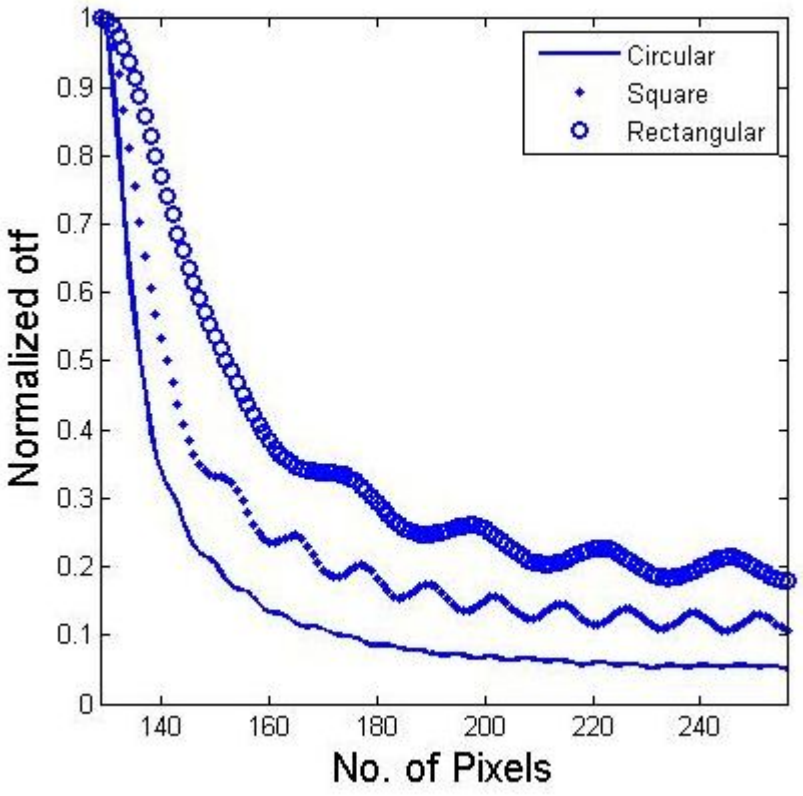

Figure 5 - Central lines of the normalized *otf* for different diffracted apertures at the same dimension of (20 pixels)

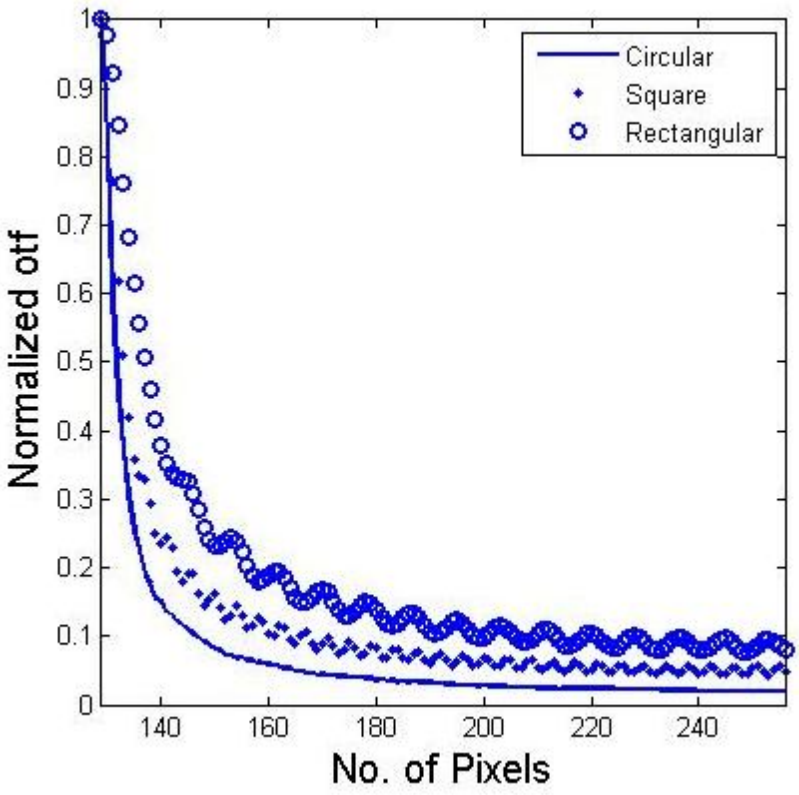

Figure 6 - Central lines of the normalized *otf* for different diffracted apertures at the same dimension of (60 pixels)

4. Conclusions:

Several important points could be concluded from the results of this studying:-

1. The circular aperture makes the high frequency components vanish approximately to zero. This means that all information that belongs to the point source entered the aperture, while the others apertures (square & rectangular) truncated these frequency components as demonstrated in figures (1, 2, and 3).
2. The minimum values of the normalized irradiance increases with increases the dimension of these apertures, but the smallest values have been calculated refers to the circular aperture (according to equation (14)) and equal to (3.1×10^{-7}) at (R = 20 pixels) , while equal to (1.0×10^{-8}) at (R = 60 pixels).
3. *otf* plays an important rule that control on the efficiency of the optical imaging systems where the smoothness of the *otf* is directly proportional to increase the dimension of the apertures, but *otf* for the circular aperture more smooth than the others. This means that the high resolution of the circular aperture.
4. *otf* is sharply decline with increases the dimensions of these apertures, but *otf* for the circular aperture becomes lower than another apertures. This gives advantage for the circular aperture in a high resolution image, as shown in figures (5 and 6).

5. References:

1. Lv, X., Liu, L., Yan, A., Li, B., Dai, E., and Sun, J. **2012**. Design and Simulation of a High Resolution Active Imaging Technique Utilizing Fresnel Telescopy. *Optik Journal*, 123, pp: 796 – 799.
2. Malacara, D., Malacara, Z. **2004**. *Handbook of Optical Design*. Second Edition. Marcel Dekker, Inc, USA. pp: 244.
3. Ersoy, O. **2007**. *Diffraction, Fourier Optics and Imaging*. John Wiley & Sons, Canada. pp: 41.

4. Estaban, D., Sosa, S. and T,oro, L. **2011**. Understanding the Physical Optics Phenomena by using a Digital Application for Light Propagation. *Journal of Physics*, 274. pp: 1- 12.
5. Möller, K. **2007**. *Optics Learning by Computing, with Model Examples using Mathcad, MATLAB, Mathematica, and Maple*. Second Edition, Springer Science + Business Media, USA. pp: 136 – 137.
6. Maurer, L. **2013**. Simulating Interference and Diffraction in Instructional Laboratories. *Physical Education Journal*, 48(2), pp: 227 – 232.
7. Lipson, A., Lipson, S., Lipson, H. **2011**. *Optical Physics*. Fourth Edition. CAMBRIDGE UNVERSITY PRESS. New York. pp: 230.
8. Mohammed, A.T. **2007**. Limits of the Efficiency of Imaging with Obstructing Apertures. *SQU: Sultan Qaboos University Journal for Science*, 12(1), pp: 67-74.
9. Saleh, B. Teich, M. **1991**. *Fundamental of Photonics*. John Wiley & Sons, Canada. pp: 127 – 128.
10. Voelz, D. **2011**. *Computational Fourier Optics.* Society of Photo – Optical Instrumentation Engineers (SPIE), USA. pp: 50 – 55.
11. Saha, S. **2007**. *Diffraction – limited Imaging with Large and Moderate Telescopes*. World Scientific Publishing Co., Singapore. pp: 123.
12. Britton, T. R. **2009**. High Dynamic Range Direct Imaging of Exoplanets with an Off-Axis Antarctic Telescope. M.Sc.Thesis. School of Physics. University of New South Wales. PP: 26 – 27.
13. Kasdin, N., Vanderlbel, R., Spergel, D. and Littman, M. **2003**. Extrasolar Planet Finding Via Optimal Apodized-Pupil and Shaped-Pupil Coronagraphs. *The Astrophysical Journal*. 582. pp :1147 – 1161.
14. Goodman , J. W. **2000**. *Statistical Optics*. John Willy & Sons. Inc. New York. PP: 169 – 171.